

1973

# Time-Dependent Radiative Cooling of a Hot Low-Density Cosmic Gas

Menas Kafatos

Chapman University, [kafatos@chapman.edu](mailto:kafatos@chapman.edu)

Follow this and additional works at: [http://digitalcommons.chapman.edu/scs\\_articles](http://digitalcommons.chapman.edu/scs_articles)

 Part of the [Stars, Interstellar Medium and the Galaxy Commons](#)

---

## Recommended Citation

Kafatos, M. (1973) Time-Dependent Radiative Cooling of a Hot Low-Density Cosmic Gas, *Astrophysical Journal*, 182:433-447. doi: 10.1086/152151

This Article is brought to you for free and open access by the Science and Technology Faculty Articles and Research at Chapman University Digital Commons. It has been accepted for inclusion in Mathematics, Physics, and Computer Science Faculty Articles and Research by an authorized administrator of Chapman University Digital Commons. For more information, please contact [laughtin@chapman.edu](mailto:laughtin@chapman.edu).

---

# Time-Dependent Radiative Cooling of a Hot Low-Density Cosmic Gas

## **Comments**

This article was originally published in *Astrophysical Journal*, volume 182, in 1973. DOI: [10.1086/152151](https://doi.org/10.1086/152151)

## **Copyright**

IOP Publishing

## TIME-DEPENDENT RADIATIVE COOLING OF A HOT LOW-DENSITY COSMIC GAS

MINAS KAFATOS

Joint Institute for Laboratory Astrophysics, University of Colorado, Boulder

*Received 17 November 1972*

### ABSTRACT

Detailed calculations are presented for the radiative cooling of a hot ( $10^4 \text{ }^\circ\text{K} \leq T \leq 10^6 \text{ }^\circ\text{K}$ ) interstellar gas. Below  $10^6 \text{ }^\circ\text{K}$  such a gas is not in ionization equilibrium because it is cooling faster than it is recombining. The gas is more ionized at a particular temperature and emits harder radiation than a gas in equilibrium at the same temperature. Optical forbidden lines, particularly the [O II], [O III] lines, are much stronger than the hydrogen Balmer lines. Hydrogen lines, if observable, would show a Balmer decrement not very different from that of a radiatively excited nebula. Results are presented in three cases: the first two have initial conditions determined when a 40- or 100-eV photon burst suddenly ionizes the gas, corresponding to a "fossil Strömgren sphere" suddenly formed by an ultraviolet or soft X-ray supernova burst. In the third case the gas is cooling from steady-state ionic abundances at  $10^6 \text{ }^\circ\text{K}$  (e.g., a supernova shell that has reached the late radiative-cooling stage).

*Subject headings:* interstellar matter — supernovae

### I. INTRODUCTION

Various workers (Cox and Tucker 1969; Allen and Dupree 1969; House 1964; Tucker and Gould 1966) have calculated the ionization equilibria for elements in a low-density cosmic gas. In all the above calculations it is assumed that electron recombinations balance collisional ionizations by thermal electrons, so that the ionic abundances are a function of the electron temperature alone. If  $Z$  denotes the nuclear charge and  $z$  the charge of one of its ions ( $z \leq Z$ ), then the ion number densities can be found from the relations

$$\frac{n_{Z,z-1}}{n_{Z,z}} = \frac{\alpha_{Z,z}(T)}{C_{Z,z-1}(T)} \quad (1)$$

where  $\alpha_{Z,z}(T)$  denotes the total recombination coefficient of element  $Z$  of ionic stage  $z$  recombining to stage  $z - 1$  at temperature  $T$ , while  $C_{Z,z-1}(T)$  denotes the collisional ionization coefficient of element  $Z$  of ionic stage  $z - 1$  ionized to the next stage  $z$  at temperature  $T$ . The parameters entering equation (1) were reviewed by Cox and Tucker (1969). The results of Cox and Tucker are expected to be more accurate because they use improved coefficients.

Once the ionic abundances are determined, the radiative cooling rate, denoted by  $\Lambda(T)$ , can be calculated by summing over all radiative processes: bremsstrahlung, recombination radiation, and line emission resulting from electron impact excitation.  $\Lambda(T)$  has been calculated by Cox and Tucker (1969) in the range  $10^4 \text{ }^\circ\text{K}$ – $10^8 \text{ }^\circ\text{K}$ , and by Tucker and Koren (1971) in the range  $10^6 \text{ }^\circ\text{K}$ – $10^8 \text{ }^\circ\text{K}$ .

Equations (1) (for steady-state, denoted hereafter as SS) imply that transient effects are not important. This is justified if recombinations and ionizations take the gas to the SS condition before cooling can appreciably lower the temperature. But when one compares the various relevant time scales, one finds that the cooling time is comparable or short compared to the relevant recombination times for  $T \lesssim 10^6 \text{ }^\circ\text{K}$ ; it follows that the SS assumption is not good if the gas is cooling radiatively below  $10^6 \text{ }^\circ\text{K}$ .

On the other hand, even above  $10^6$  ° K if the gas cools by some other means (e.g., loss of heat by expansion or by conduction), the cooling time may be comparable to or shorter than the ionization and recombination times, and SS may not hold (see Kafatos and Tucker 1972).

In the work of Cox and Tucker (1969) and Tucker and Gould (1966), the gas was assumed to be optically thin to all radiation. This point is examined below.

The time-dependent radiative cooling is treated here as generally as possible, although certain effects (e.g., recombination radiation) are ignored. Exact results depend on atomic parameters, some of which are not well known. Time-dependent radiative cooling below  $10^4$  ° K has been treated by Jura and Dalgarno (1972), Schwarz (1972), and Gerola, Iglesias, and Gamba (1973). In that temperature range hydrogen is not thermally ionized and the cooling is fundamentally different from the cooling occurring above  $10^4$  ° K.

Results for three cases are presented here.

i) A cosmic gas initially at  $10^6$  ° K and with initial ionic abundances given by SS (this is denoted hereafter as SS,  $10^6$  ° K); this case corresponds to a hot gas that has reached the radiative cooling stage, e.g., a supernova shell.

ii) A cosmic gas initially at  $3.3 \times 10^5$  ° K and the following relative ionic abundances:  $H^+ = 1$ ,  $He^{++} = 1$ ,  $C^{+4} = 1$ ,  $O^{+4} = 1$ ,  $Ne^{+4} = 1$ . Such initial conditions are expected if the gas is suddenly ionized by a 100-eV soft X-ray supernova burst<sup>1</sup> (Schwarz 1972). We refer to this case as 100 eV.

iii) A cosmic gas initially at  $10^5$  ° K and with the following relative ionic abundances:  $H^{+1} = 1$ ,  $He^+ = 1$ ,  $C^{+2} = 1$ ,  $O^{+2} = 1$ ,  $Ne^+ = 1$ . Such initial conditions are expected if the gas is suddenly ionized by a 40-eV ultraviolet supernova burst (Morrison and Sartori 1969; Kafatos and Morrison 1971; Kafatos 1971). We refer to this case as 40 eV.

All results are given for  $n_0 = 1 \text{ cm}^{-3}$ , where  $n_0$  is the sum of the densities of the hydrogen and helium nuclei;  $n_0$  is constant (isochoric case) if the cooling time  $T/(dT/dt)$  is short compared to the hydrodynamic time  $t_p \sim 2R/V_s$ , where  $V_s$  is the sound velocity and  $R$  the radius of the cooling region. This is certainly true if the radius is larger than a fraction of a parsec for the temperature range considered in the present paper. The "fossil Strömgren spheres" (Brandt *et al.* 1971), denoted by FSS, examined here have radii in the neighborhood of 100 pc. Therefore,  $n_0$  is taken to be constant; for other densities note that the transformation  $n_0' = \lambda n_0$ ,  $t' = \lambda^{-1}t$ , where  $t$  is the time, holds.

## II. EQUATIONS

The time-dependent treatment replaces equations (1) by the set of equations

$$\begin{aligned} \frac{dn_{H^+}}{dt} &= C_{1,0}n_en_{H^0} - \alpha_{1,1}n_en_{H^+}, \dots, \\ \frac{dn_{Z,z}}{dt} &= C_{Z,z-1}n_en_{Z,z-1} - C_{Z,z}n_en_{Z,z} + \alpha_{Z,z+1}n_en_{Z,z+1} - \alpha_{Z,z}n_en_{Z,z}, \dots, \\ \frac{d}{dt} \left( \frac{3}{2}kTn \right) &= -n_en_H\Lambda(\dots, n_{Z,z}, \dots, T), \end{aligned} \quad (2)$$

where  $n$  is the total number density  $n = n_H + n_{He^0} + n_{He^+} + n_{He^{++}} + n_e$  and  $n_H$  is the total hydrogen number density.

<sup>1</sup> We limit ourselves to the fully ionized zone, even though an appreciable partially ionized transition region is formed in a soft X-ray burst.

### a) The Ionization-Balance Equations

In this work the following ions were included:  $H^+$ ,  $He^0$ ,  $He^+$ ,  $He^{++}$ ,  $C^0$ - $C^{+6}$ ,  $O^0$ - $O^{+7}$ ,  $Ne^0$ - $Ne^{+8}$ , resulting in a total of 28 equations. Nitrogen can be ignored (because of its low cosmic abundance). It is assumed in equations (2) that the only ionizing agent is collisions with thermal electrons, and that the ions recombine via dielectronic and radiative transitions. The collisional ionization rate coefficient  $C_{Z,z}$  is calculated from the approximation of Cox and Tucker (1969) to the Lotz (1967) values. The recombination coefficient  $\alpha_{Z,z}$  is the sum of the radiative coefficient  $\alpha_{Z,z}^R$  and the dielectronic recombination coefficient  $\alpha_{Z,z}^D$ .

Cox and Tucker (1969) calculated the radiative recombination coefficient  $\alpha_{Z,z}^R$ . Their results can be written in the form

$$\alpha_{Z,z}^R = \alpha_z^R f_{Z,z}(T), \quad (3)$$

where  $\alpha_z^R$  is the hydrogenic formula of Seaton (1959) and  $f_{Z,z}(T)$  a slowly varying function of  $T$ . Values of  $f$  range from 0.35 to 1.75 for  $10^3 < T < 10^7$  °K. I chose appropriate mean values of  $f$  in the temperature range where each ion  $Z, z$  makes a significant contribution. Agreement to better than 35 percent with the Cox and Tucker results was obtained. Values of  $f$  were kindly provided to me by Dr. W. Tucker. There is some uncertainty in the calculations of  $\alpha_{Z,z}^R$  (cf. Tarter 1971), and the results sensitively depend on the values of the radiative recombination coefficients used.

The dielectronic recombination coefficient  $\alpha_{Z,z}^D$  was calculated from the formula of Burgess (1965), using the values of the oscillator strength and the energy of transition given by Wiese, Smith, and Glennon (1966).

Finally the following particle-conservation equations hold:

$$\begin{aligned} n_H &= n_{H^0} + n_{H^+} = \frac{1}{1+a} n_0, \\ n_{He^0} + n_{He^+} + n_{He^{++}} &= \frac{a}{1+a} n_0, \\ n_e &= n_{H^+} + n_{He^+} + 2n_{He^{++}}, \\ n &= n_{H^0} + n_{H^+} + n_{He^0} + n_{He^+} + n_{He^{++}} + n_e = n_0 + n_e, \end{aligned} \quad (4)$$

where  $a$  is the ratio of the abundance of helium to hydrogen taken to be 0.16 and  $n_0$  is the constant sum of the densities of the hydrogen and helium nuclei (isochoric case). In equations (4) the contribution of the heavy ions to the electron density is ignored.

### b) The Question of Optical Thickness

We must consider how photoionization by line and continuum affect the ionization balance. We consider hot, fully ionized regions of characteristic size  $R$ . These regions are cooling radiatively and are formed in a photoionizing supernova burst (a fossil Strömgren sphere). The size  $R$  is  $\sim 100$  pc (40-eV case) and  $\sim 50$  pc (100-eV case) for a total number of ionizing photons  $10^{62}$  and  $n_0 = 1 \text{ cm}^{-3}$ .

In the case of the heavy elements (other than H, He) the optical depth is less than unity for both continuum and resonance radiation even at line center.

In the case of hydrogen the mean free path of the Lyman continuum radiation is likely to be much smaller than  $R$  when appreciable amounts of neutral hydrogen exist. In order to account for the photoionization of hydrogen by recombination continuum we ignore recombinations to the ground state and use only  $\alpha^{(2)}$  (Spitzer 1968). However, we find *a posteriori* that a 50–100 pc region becomes optically thin to the Lyman

continuum for  $T \gtrsim 35,000^\circ \text{K}$ . Therefore, we use the approximation of using  $\alpha^{(2)}$  for  $T < 35,000^\circ \text{K}$  (cases A and B, respectively, of Menzel 1937).

Line and continuum radiation from helium (Jura and Dalgarno 1972) can photoionize hydrogen and hence reduce the effective recombination of hydrogen. This effect, however, is less than 20 percent of that due to direct hydrogen recombination for  $T > 15,000^\circ \text{K}$  and was ignored here.

On the other hand, these processes cannot be ignored in the ionization balance of helium, since they contribute terms of the same order of magnitude as those already included in equations (2) for  $T \lesssim 50,000^\circ \text{K}$ . However, at those temperatures helium influences system (2) through  $n_e$  only, and the inclusion of these terms would change  $n_e$  by at most 14 percent. Therefore, these terms were ignored.

Finally the contribution of hydrogen and helium to the opacity of the radiation emitted by the heavy elements is small.

### c) The Energy-Balance Equation

The ionization-balance equations in (2) are coupled with the last equation which describes the evolution of the temperature with time. If only hydrogen is considered in the total density, this equation is

$$\frac{3k}{2} n_0(1+x) \frac{dT}{dt} = -n_0^2 \Lambda' - \left(\frac{3}{2}kT + I_{\text{H}}\right) n_0 \frac{dx}{dt}, \quad (5)$$

where  $\Lambda'$  is the cooling rate due to all radiation,  $x$  the ionized fraction of hydrogen, and  $I_{\text{H}}$  is the ionization potential of hydrogen. This equation can be easily generalized to include helium. The  $dx/dt$  term which does not occur in steady state should be included whenever the recombination radiation is included in  $\Lambda'$ , since they are of the same order of magnitude. Photoelectrons resulting from helium excitations and recombinations provide a heat source that persists after the initial ionizing flash (Jura and Dalgarno 1972). These heat terms and time-dependent terms in helium—analogueous to the  $dx/dt$  term in hydrogen—contribute at most  $5 \times 10^{-25}/n_0^2 \text{ erg cm}^3 \text{ s}^{-1}$  at  $T \sim 10^4 \text{ }^\circ \text{K}$ . It follows that helium may be included in the energy-balance equation only through  $n$  and  $n_e$  without important loss of accuracy. When this is done, the energy-balance equation takes the form

$$\frac{3kn}{2} \frac{dT}{dt} = -\Lambda n_e n_{\text{H}} - D + A - B - (C), \quad (6)$$

where

$$\Lambda = \Lambda' - \mathcal{L}_{\text{Rec}}^{\text{H}}, \quad \mathcal{L}_{\text{Rec}}^{\text{H}} = \int \sigma v (I_{\text{H}} + E) f(v) dv.$$

Here  $f(v)$  is the Maxwellian distribution,  $\langle \sigma v \rangle$  is the total recombination coefficient  $\alpha^{(1)} \equiv \alpha_{1,1}$  and

$$\langle E_{\text{r}} \rangle_{\text{H}} = \frac{\int E f(v) \sigma(v) v dv}{\langle \sigma v \rangle};$$

also

$$\begin{aligned} A &= \frac{3}{2}kT \alpha^{(1)} n_e n_{\text{H}^+}, & B &= \langle E_{\text{r}} \rangle_{\text{H}} \alpha^{(1)} n_e n_{\text{H}^+}, \\ C &= \frac{3}{2}kT \langle \sigma_1 v \rangle - \langle E \sigma_1 v \rangle, & D &= \left(\frac{3}{2}kT + I_{\text{H}}\right) C_{1,0}(T) n_e n_{\text{H}}^0, \end{aligned}$$

where  $\sigma_1$  denotes the cross-section for recombination to the ground state. The term (C) was included when the gas was optically thick to the Lyman continuum. The sum

of all the terms other than the  $\Lambda$  term, in the right-hand side of equation (6), is negative above  $\sim 20,000^\circ \text{K}$  (collisions of electrons with  $\text{H}^0$  atoms remove the highest-energy electrons; i.e., we have cooling), while below about  $20,000^\circ \text{K}$  recombination is the dominant term and their sum becomes positive (the lowest-energy electrons are removed first by recombination, and the mean energy increases). Note that the  $D$  term in equation (6) has a strong peak around  $40,000^\circ \text{K}$ , while the rest slowly decrease absolutely with decreasing  $T$ . The  $A$ ,  $B$ , and  $C$  terms arise from recombinations while the  $D$  term is due to collisions, arising from the term containing  $dn_{\text{H}^+}/dt$ .

The radiative cooling function  $\Lambda$  is sensitive to the element abundances chosen. For example, if solar abundances (cf. Withbroe 1971) are used, the cooling time increases by a factor of 2.4 with respect to the cooling time if cosmic abundances (cf. Aller 1961) are used. In this study the cosmic abundances of Aller are used.

The heated medium cools predominantly by electron-impact excitations of  $\text{H}$ ,  $\text{He}^0$ ,  $\text{He}^+$ , and the heavy ions. At high temperatures (above  $30,000^\circ \text{K}$ ) the predominant cooling occurs from electron-impact excitations of levels that radiate back to the ground term via allowed transitions (Tucker and Gould 1966; Cox and Tucker 1969; Cox and Daltabuit 1971). I used the formula found in Cox and Tucker for this process. Values of the Gaunt factor were taken from Cox (1970), while values of the oscillator strength and energy of transition were taken from Wiese *et al.* (1966). I included 69 terms arising from the various levels of the ionic stages of  $\text{He}^0$ ,  $\text{He}^+$ ,  $\text{C}^+ - \text{C}^{+5}$ ,  $\text{O}^+ - \text{O}^{+7}$ ,  $\text{Ne}^+ - \text{Ne}^{+8}$ . Nitrogen was ignored because of its relatively low abundance; however, it should be included if solar abundances are used. The contribution of  $\text{Mg}$ ,  $\text{Si}$ , and  $\text{S}$  to  $\Lambda$  is dominant only around  $10^6^\circ \text{K}$ . I used power-law approximations to this contribution found in Cox and Tucker (1969). The ions of  $\text{Mg}$ ,  $\text{Si}$ , and  $\text{S}$  are expected to be close to their SS values due to their fast recombination.

The region also cools due to excitations of metastable and fine-structure levels of various heavy ions. At high temperatures ( $> 10^4^\circ \text{K}$ ) the excitation of the metastable levels is more important, while at lower temperatures ( $< 10^4^\circ \text{K}$ ) the excitation of fine-structure levels is more important. I included nine terms arising from forbidden and semiforbidden transitions in the following ions:  $\text{C}^+$ ,  $\text{C}^{+2}$ ,  $\text{O}^+ - \text{O}^{+4}$ , and  $\text{Ne}^{+2} - \text{Ne}^{+4}$ . These terms are significant from  $10^4^\circ \lesssim T \lesssim 5 \times 10^4^\circ \text{K}$ , and the relevant parameters were taken from Jura and Dalgarno (1972). The fine-structure terms are negligible for  $T > 10^4^\circ \text{K}$ .

The cooling due to collisional excitation of allowed levels in neutral hydrogen is important below about  $30,000^\circ \text{K}$ . The formula used for this cooling is due to Bottcher (cf. Jura 1971).

Bremsstrahlung, radiative, and dielectronic recombination radiation make a negligible contribution to  $\Lambda$  below  $10^6^\circ \text{K}$ .

#### d) Time Scales

In order to estimate circumstances under which departures from SS are important we define the following time scales:

a) The collisional ionization time for an ionic stage  $Z, z$

$$t_I^{Z,z} = (C_{Z,z} n_e)^{-1}.$$

b) The recombination time for an ionic stage  $Z, z$

$$t_R^{Z,z} = (\alpha_{Z,z} n_e)^{-1}.$$

c) The cooling time

$$t_c = T / (dT/dt).$$

The region may be cooling by radiation alone or by some other process.

We are only concerned with what happens after the ions and electrons in the gas have reached a common "initial" temperature  $T_i$ . This time is a few years for  $n_0 = 1$  and  $10^5 \text{ }^\circ \leq T \leq 10^6 \text{ }^\circ \text{K}$ .

If  $t_c \gg (t_R, t_I)$  in the most abundant species, the gas is in steady state (SS) and equations (1) hold. This happens above  $\sim 10^6 \text{ }^\circ \text{K}$  for the elements of concern. Table 1 gives  $t_R^{z,z}, t_I^{z,z}$  for the most important oxygen ions and  $t_c$  in the temperature range  $10^5 \text{ }^\circ - 10^6 \text{ }^\circ \text{K}$ . Examining table 1, one can see what happens to an ionic state  $z$  as  $T$  changes. The recombination time has a minimum if dielectronic recombination is important; otherwise it increases with  $T$  as  $1/(\alpha_{z,z}^R)$ . As  $T \rightarrow 0$  or  $T \rightarrow \infty, \alpha_{z,z} \rightarrow \alpha_{z,z}^R$ ; also  $t_I^{z,z}$  increases as  $T$  decreases. Therefore, a time comes when  $t_I^{z,z}$  and  $(n_e \alpha_{z,z}^D)^{-1}$  are appreciably greater than  $t_c$ . From then on the ion  $z$  recombines only by radiation to  $z - 1$ . Since radiative recombination is relatively slow (compared to dielectronic recombination when the latter is maximum), it follows that as the temperature drops the higher stage of ionization will be overabundant compared to SS at the same  $T$ . Departures from SS will be greater for the ions that recombine primarily by radiation for any  $T$ , namely, the helium-like ions C v, O vii, Ne ix, and the corresponding hydrogenic ions.

In the case of hydrogen the following situation holds:  $t_c$  is always less than  $t_R^H$  and  $t_I^H > t_c$  below  $\sim 20,000 \text{ }^\circ \text{K}$ . But below  $20,000 \text{ }^\circ \text{K}$  the SS abundance of  $H^0$  becomes important. It follows that the temperature drops to  $10^4 \text{ }^\circ \text{K}$  before any appreciable recombination of hydrogen occurs. At  $T = 10^4 \text{ }^\circ \text{K}$  hydrogen is still mostly ionized (93 percent). Above  $30,000 \text{ }^\circ \text{K}$  any appreciable departure from SS in the abundance of  $H^+$  quickly disappears due to the large collisional-ionization term. The SS value is reached within a time of the order of  $t_I^H$ .

We now turn to specific solutions of the time-dependent system (2).

TABLE 1  
IONIZATION AND RECOMBINATION TIMES FOR OXYGEN AND COOLING TIME  
IN THE RANGE  $10^5 \text{ }^\circ - 10^6 \text{ }^\circ \text{K}$

z	T (°K)					
	10 <sup>5</sup>	2 × 10 <sup>5</sup>	3 × 10 <sup>5</sup>	5 × 10 <sup>5</sup>	7 × 10 <sup>5</sup>	10 <sup>6</sup>
	<i>t<sub>R</sub><sup>z,z</sup> (sec)</i>					
2.....	6.5 × 10 <sup>10</sup>	3.5 × 10 <sup>10</sup>	3.46 × 10 <sup>10</sup>	5.8 × 10 <sup>10</sup>	9.7 × 10 <sup>10</sup>	2.5 × 10 <sup>11</sup>
3.....	4.27 × 10 <sup>10</sup>	1.9 × 10 <sup>10</sup>	1.9 × 10 <sup>10</sup>	3.4 × 10 <sup>10</sup>	5.5 × 10 <sup>10</sup>	10 <sup>11</sup>
4.....	4.2 × 10 <sup>10</sup>	1.53 × 10 <sup>10</sup>	1.5 × 10 <sup>10</sup>	1.95 × 10 <sup>10</sup>	3.14 × 10 <sup>10</sup>	6.5 × 10 <sup>10</sup>
5.....	3.75 × 10 <sup>11</sup>	2.66 × 10 <sup>10</sup>	2.76 × 10 <sup>10</sup>	3.88 × 10 <sup>10</sup>	4.5 × 10 <sup>10</sup>	5.92 × 10 <sup>10</sup>
6.....	2.52 × 10 <sup>11</sup>	4.7 × 10 <sup>11</sup>	4.9 × 10 <sup>11</sup>	7.74 × 10 <sup>11</sup>	9.1 × 10 <sup>11</sup>	1.1 × 10 <sup>12</sup>
7.....	1.36 × 10 <sup>11</sup>	2.2 × 10 <sup>11</sup>	2.88 × 10 <sup>11</sup>	4.15 × 10 <sup>11</sup>	4.7 × 10 <sup>11</sup>	6.7 × 10 <sup>11</sup>
8.....	8.5 × 10 <sup>10</sup>	1.35 × 10 <sup>11</sup>	1.8 × 10 <sup>11</sup>	2.55 × 10 <sup>11</sup>	3.24 × 10 <sup>11</sup>	4.2 × 10 <sup>11</sup>
	<i>t<sub>I</sub><sup>z,z</sup> (sec)</i>					
1.....	5.25 × 10 <sup>9</sup>	4.85 × 10 <sup>8</sup>	2 × 10 <sup>8</sup>	9.1 × 10 <sup>7</sup>	6.05 × 10 <sup>7</sup>	4.25 × 10 <sup>7</sup>
2.....	1.1 × 10 <sup>11</sup>	3.26 × 10 <sup>9</sup>	9.2 × 10 <sup>8</sup>	3.36 × 10 <sup>8</sup>	1.79 × 10 <sup>8</sup>	1.14 × 10 <sup>8</sup>
3.....	3.22 × 10 <sup>12</sup>	2.55 × 10 <sup>10</sup>	4.65 × 10 <sup>9</sup>	1.1 × 10 <sup>9</sup>	5.52 × 10 <sup>8</sup>	3.14 × 10 <sup>8</sup>
4.....	4.84 × 10 <sup>14</sup>	4.6 × 10 <sup>11</sup>	4.16 × 10 <sup>10</sup>	5.53 × 10 <sup>9</sup>	2.2 × 10 <sup>9</sup>	1.04 × 10 <sup>9</sup>
5.....	2.6 × 10 <sup>16</sup>	6.12 × 10 <sup>12</sup>	3.46 × 10 <sup>11</sup>	3.17 × 10 <sup>10</sup>	1.1 × 10 <sup>10</sup>	4.54 × 10 <sup>9</sup>
6.....	5.7 × 10 <sup>17</sup>	10 <sup>28</sup>	5.11 × 10 <sup>22</sup>	4.33 × 10 <sup>17</sup>	2.73 × 10 <sup>15</sup>	5.83 × 10 <sup>13</sup>
7.....	8.3 × 10 <sup>54</sup>	6.9 × 10 <sup>32</sup>	2.77 × 10 <sup>25</sup>	3.05 × 10 <sup>19</sup>	8.04 × 10 <sup>16</sup>	8.86 × 10 <sup>14</sup>
<i>t<sub>c</sub> (sec).....</i>	1.3 × 10 <sup>11</sup>	1.9 × 10 <sup>11</sup>	3.4 × 10 <sup>11</sup>	8 × 10 <sup>11</sup>	2.16 × 10 <sup>12</sup>	5.87 × 10 <sup>12</sup>

NOTE.—The cooling time  $t_c$  is shown if the gas cools from  $10^6 \text{ }^\circ \text{K}$  and SS initial abundances.



## III. RESULTS

## a) Radiative Energy Loss

Figure 1 shows the radiative energy loss  $P/n_0^2$  ( $\text{erg cm}^3 \text{s}^{-1}$ ): curve *A* is the steady-state curve (cf. Cox and Tucker 1969), while curve *B* the time-dependent curve found by the complete solution of equations (2). The initial ionic abundances for curve *B* are the same as for curve *A* (SS) at  $T = 10^6$  ° K. The peaks due to the ions of Ne, O, C, and H in the SS curve are appreciably reduced (especially for hydrogen) in curve *B* because the most important cooling agents that give rise to each peak are underabundant at the temperature where their contribution to the cooling is maximum.

Figure 2 shows the time derivative of the temperature in three different cases (all by solving system [2]): curve *C* is the SS,  $10^6$  ° K case (see Introduction), curve *B* is the 100-eV case, while curve *A* is the 40-eV case; time-dependent cooling is not necessarily less than the SS cooling; curves *A* and *B* are higher than the SS  $dT/dt$  curve due to the initial conditions chosen; after some time, though, recombination takes its toll and they become less than the SS curve. Note that the system effectively loses all memory of the initial conditions below  $20,000$  ° K, as far as the cooling curve is concerned; however, individual line strengths are different in the three cases even at  $T = 10^4$  ° K.

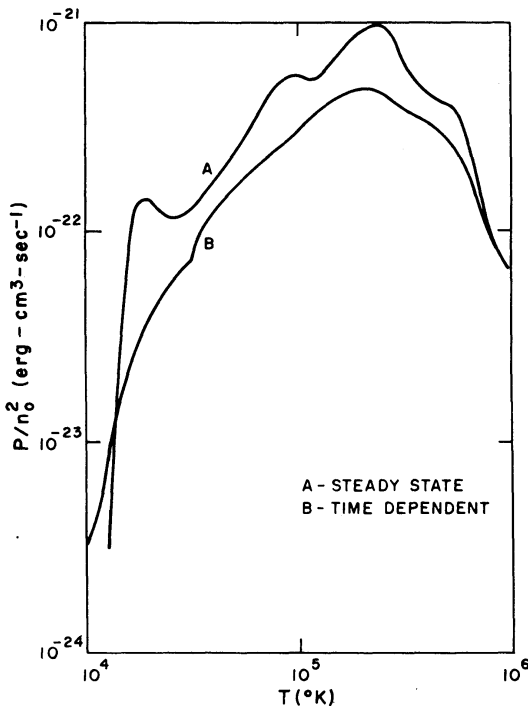


FIG. 1

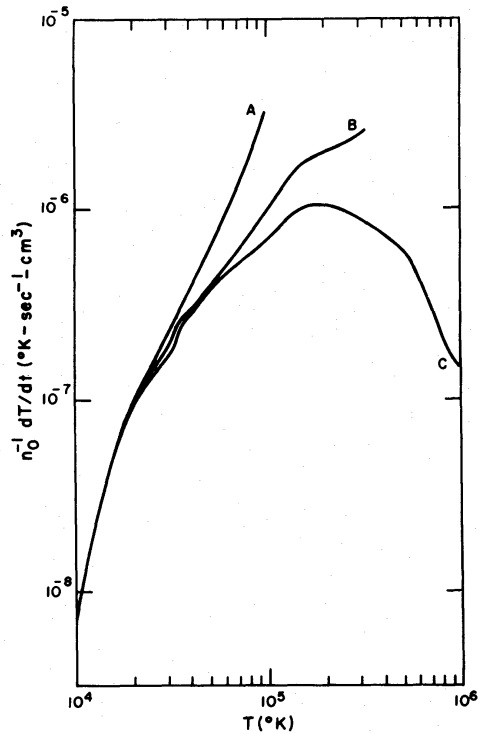


FIG. 2

FIG. 1.—Radiative energy loss is shown here. Curve *A* is the SS curve; curve *B*, the time-dependent curve found by solving the complete system (2). Both curves have the same initial abundances, namely, the SS abundances at  $T = 10^6$  ° K.

FIG. 2.—The time derivative of the temperature for three different cases. Curve *A* is the 40-eV photon burst case, curve *B*, the 100-eV photon burst case; curve *C* is the case if the initial conditions are given by the SS theory at  $10^6$  ° K. One should multiply by  $n_0$  to obtain  $dT/dt$ .

Time dependent cooling does not differ appreciably from SS cooling because neighboring stages of ionization have comparable line emissivities. Around the temperature at which an ionization stage  $z$  reaches its maximum, the derivative  $dn_{z,z}/dt$  changes fastest, tending to make the  $z$  abundance go to its SS value, or at least one of the next stages  $z - 1, z + 1$ .

### b) The Ionic Abundances

In figures 3–6 the calculations for H, He, C, O, and Ne are presented in the form  $n_{z,z}/n_z$  (the ionized fraction, where  $n_z = \sum_{\text{all } z} n_{z,z}$ ) versus time. The abundances of  $C^0, O^0$  are actually much smaller than shown, because  $C^0$  is photoionized by starlight in the interstellar medium and  $O^0$  is depleted due to the fast reaction (Field and Steigman 1971)  $O^+ + H^0 \rightleftharpoons O^0 + H^+$ . These effects only increase the abundances of  $C^+$  and  $O^+$  by about 20 and 10 percent, respectively, at  $10^4$  ° K. In all these graphs the temperature  $T$  is also shown. The initial conditions for all are given by the SS,  $10^6$  ° K case (in these figures  $t$ , the time, has been shifted to show the most important results; i.e., the H, He results are shown for  $T < 3.3 \times 10^5$  ° K and the rest for  $T < 8.5 \times 10^5$  ° K). The higher ionization stages recombine to lower ones, and eventually (when  $T = 10^4$  ° K) only the lowest stages are abundant. However, we notice that the qualitative behavior of all ionic stages is not the same: the highest ones— $C^{+5}$  and  $C^{+6}, O^{+6}$  and  $O^{+7}, Ne^{+8}$ —decrease continuously, i.e., they always recombine to the next lowest stages, while the lowest stages— $C^0, C^+, O^0, O^+, Ne^0, Ne^+$ —increase continuously, i.e., the next highest stage always recombines to them;

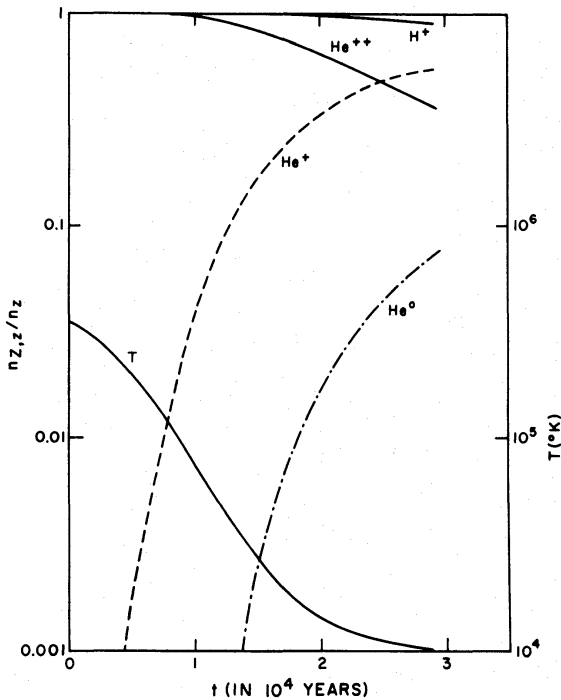


FIG. 3

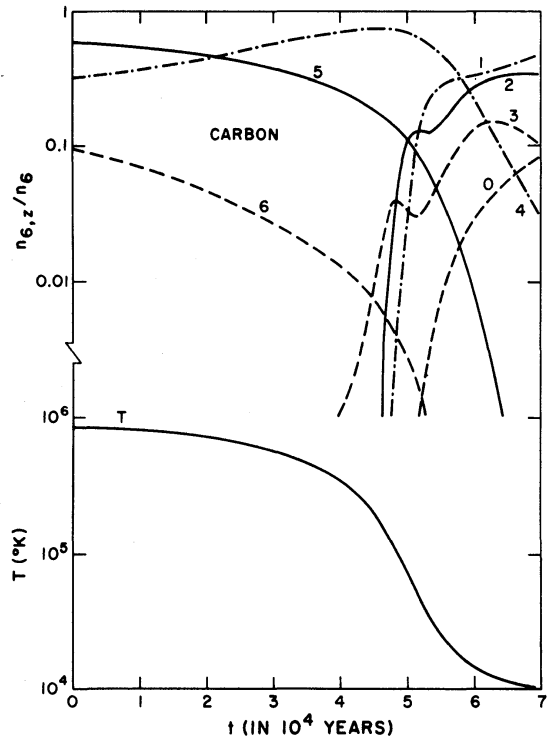


FIG. 4

FIG. 3.—Temperature and relative ionic abundances of H, He as a function of time, in  $10^4$  years. The initial conditions are given by the SS theory at  $10^6$  ° K.

FIG. 4.—Same as fig. 3 for C.

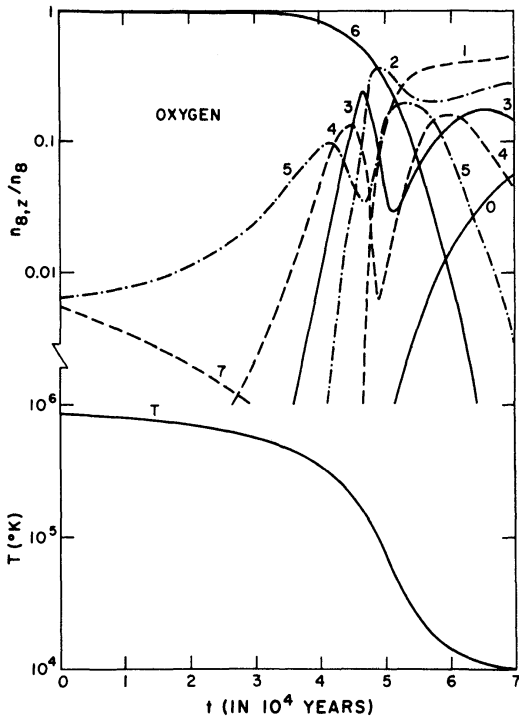


FIG. 5

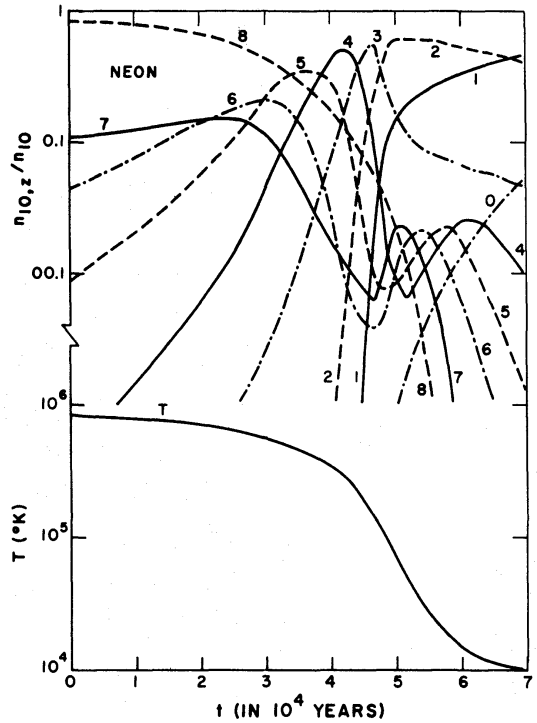


FIG. 6

FIG. 5.—Same as fig. 3 for O  
 FIG. 6.—Same as fig. 3 for Ne

the intermediate stages have two peaks. To illustrate this behavior we examine a typical intermediate ionic stage, for instance  $O^{+5}$  (fig. 5). In the range  $T \gtrsim 3 \times 10^5$  °K radiative recombination of  $O^{+6}$  builds up the abundance of  $O^{+5}$ . In the range  $1.5 \times 10^5 \text{ } \lesssim T \lesssim 3 \times 10^5$  °K dielectronic recombination rapidly depletes  $O^{+5}$ . In the range  $3 \times 10^4 \text{ } \lesssim T \lesssim 1.5 \times 10^5$  °K dielectronic recombination of  $O^{+5}$  is no longer effective and again recombination of  $O^{+6}$  increases  $O^{+5}$ . Finally, for  $T \lesssim 3 \times 10^4$  °K,  $O^{+6}$  is depleted and  $O^{+5}$  recombines radiatively.

Figures 7 and 8 give  $n_{8,z}/n_8$  (the relative oxygen-ion population) versus the temperature; in the same figures (*dashed curves*)  $(n_{8,z}/n_8)_{SS}$  (the SS relative ion population) is shown. It is immediately obvious that due to the effects mentioned in § II*d* high ionic stages persist at lower temperatures where, according to SS theory, they should be nonexistent. Figures 7–8 have the same initial ionic abundances as figures 3–6.

In table 2 we present results obtained for two cases: in Case I the region is thin to the hydrogen Lyman continuum until  $T \sim 35,000$  °K, then thick to this continuum; and in Case II the region is thin to the hydrogen Lyman continuum at all times. Calculations were also made assuming the region is thick to the Lyman continuum at all times, and the results obtained are very similar to those of Case I.

Departures from the SS abundances can be observed only if the particular ion in question has observable lines at temperatures where this departure is appreciable. This is best done for the ions that have forbidden lines. A characteristic of the time-dependent treatment is that at a given  $T$  the radiation from the cooling region is harder than the corresponding radiation under SS conditions.

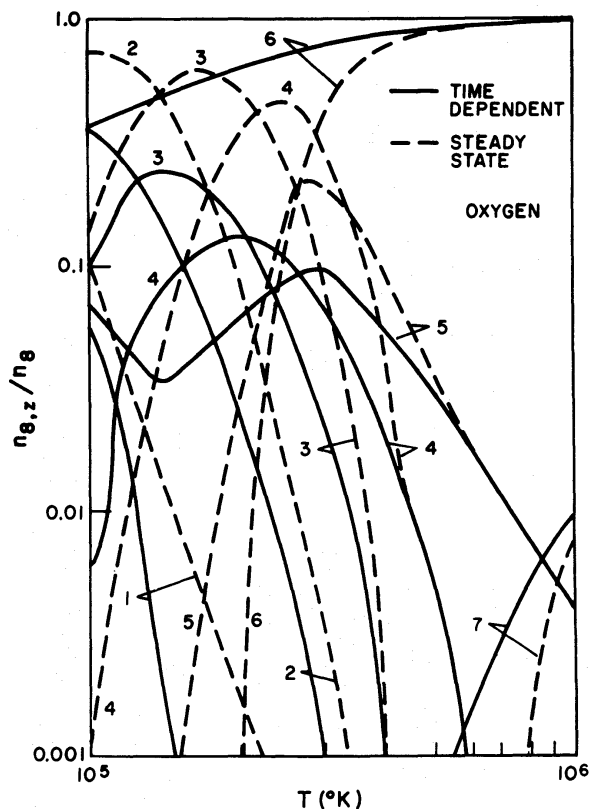


FIG. 7

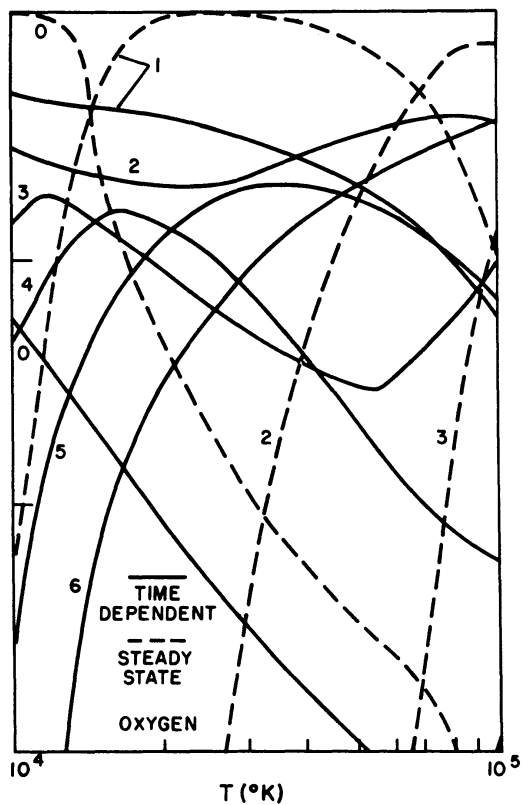


FIG. 8

FIG. 7.—Relative oxygen population as a function of  $T$  ( $10^5 \text{ }^\circ\text{K} \leq T \leq 10^6 \text{ }^\circ\text{K}$ ). The full curves give the time-dependent results; the dashed curves, the SS results. Initial conditions the same as fig. 3.

FIG. 8.—Same as fig. 7 but for  $10^4 \text{ }^\circ\text{K} \leq T \leq 10^5 \text{ }^\circ\text{K}$ .

c) Line Intensities

In this section we present results of the hydrogen-line emissivities ( $L_\alpha$ ,  $H\alpha$ ) as well as the strongest forbidden-line emissivities of a region cooling by radiation. Results are presented in the three cases (SS,  $10^6 \text{ }^\circ\text{K}$ ; 100 eV; 40 eV), although the results for hydrogen are not sensitive to the initial conditions. Results are again given in (volume emissivity)/ $n_0^2$ .

First consider the volume emissivity of  $L_\alpha$ . For collisional excitation the rate of population of a level of quantum number  $n$  diminishes rapidly as  $n$  increases (Kaplan and Pikel'ner 1971). If the nebula is thick to the Lyman continuum, it is very thick to the Lyman lines (Seaton 1960) and all the Lyman lines are degraded to  $L_\alpha$ ; one may therefore assume that only  $L_\alpha$  is emitted by the cooling region (Zanstra 1927). Most of the  $L_\alpha$  quanta escape, and in any case the propagation of  $L_\alpha$  radiation through the ionized region does not affect its thermal balance.

The  $L_\alpha$  volume emissivity is therefore

$$P_{L\alpha} = n_e n_{H^0} \langle v \sigma_{12} \rangle E_{L\alpha} + P_{L\alpha}(\text{Recomb}), \tag{7}$$

where the first term is due to the collisional excitation of the  $n = 2$  level from the ground state (the excitation of higher levels does not contribute appreciably to the emission rate),  $E_{L\alpha}$  is the energy of the  $2 \rightarrow 1$  transition, and  $P_{L\alpha}(\text{Recomb})$  is the rate

TABLE 2  
RELATIVE ION ABUNDANCE AT  $T = 10^4$  ° K

Element or Ion	Case I	Case II
H <sup>+</sup> .....	0.934	0.885
He <sup>0</sup> .....	0.157	0.142
He <sup>+</sup> .....	0.835	0.850
He <sup>+2</sup> .....	0.008	0.008
C <sup>0</sup> .....	0.150	0.137
C <sup>+</sup> .....	0.743	0.738
C <sup>+2</sup> .....	0.107	0.125
O <sup>0</sup> .....	0.078	0.070
O <sup>+</sup> .....	0.638	0.623
O <sup>+2</sup> .....	0.281	0.304
O <sup>+3</sup> .....	0.003	0.003
Ne <sup>0</sup> .....	0.092	0.083
Ne <sup>+</sup> .....	0.786	0.790
Ne <sup>+2</sup> .....	0.122	0.127

NOTE.—In Case I the gas is assumed to be thin to all radiation until  $T \simeq 35,000$  ° K; then it is thick to the Lyman continuum. In Case II the gas is thin to all radiation at all times. The initial abundances are the appropriate ones for a 40-eV burst and  $T = 10^5$  ° K.

of emission of  $L\alpha$  as a result of recombinations. When the nebula is thick to the continuum,  $P_{L\alpha}(\text{Recomb}) = \alpha^{(2)}n_e n_{H^+}$ . Note that the emission rate for all Balmer quanta (including continuum) is equal to the emission rate for  $L\alpha$  quanta. The first term in equation (7) was calculated from the Bottcher formula in Jura (1971). Figure 9 gives the  $L\alpha$  emissivity as a function of  $T$  (40-eV case); the line labeled "coll. (time depend.)" is the first term of equation (7) while the one labeled "recombin." is the second term of equation (7). In the same figure the full curve is the sum of the above two curves (eq. [7]). Also the dashed curve labeled "coll. (SS)" is the volume emissivity of  $L\alpha$  when steady state holds. Note that the line emissivity in the time-dependent case never reaches the high peak of the SS curve; this is because the abundance of  $H^0$  is less in the time-dependent case than in the SS case (slow recombination). In fact, at 18,000° K (peak of SS curve) the ratio of the time dependent to the SS emissivity is less than  $\frac{1}{10}$ ; moreover, the time-dependent peak is reached at higher temperature (40,000° K). Note that at low temperatures ( $T \lesssim 14,000$ ° K) the second term in equation (7) becomes dominant; i.e., the  $n = 2$  level is mostly populated by recombinations. Below 13,000° K the SS emissivity becomes less than the time-dependent emissivity, the latter decreasing much more slowly than the first due to the presence of the second term in equation (7).

We are next interested in the volume emissivity of  $H\alpha$ :

$$P_{H\alpha} = n_e n_{H^0} \langle v\sigma \rangle E_{H\alpha} + P_{H\alpha}(\text{Recomb}). \quad (8)$$

The first term is due to the collisional excitation of all levels that give rise to the emission of a Balmer- $\alpha$  photon: therefore, the expression  $\langle v\sigma \rangle_{\text{eff}}$  denotes an effective rate for the emission of an  $H\alpha$  photon; it can be found in the results of Parker (1964). The second term in equation (8) gives the emission rate of an  $H\alpha$  photon resulting by recombinations to all levels that subsequently cascade down to the  $n = 3$  level as well as the emission rate resulting by direct recombinations to  $n = 3$  (Seaton 1960).

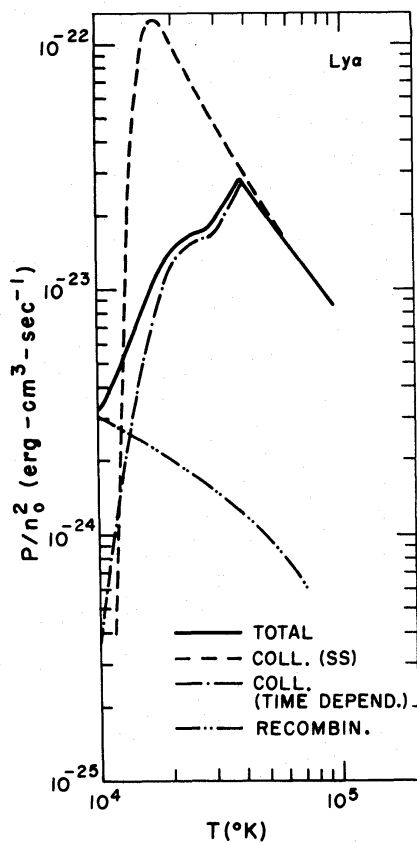


FIG. 9

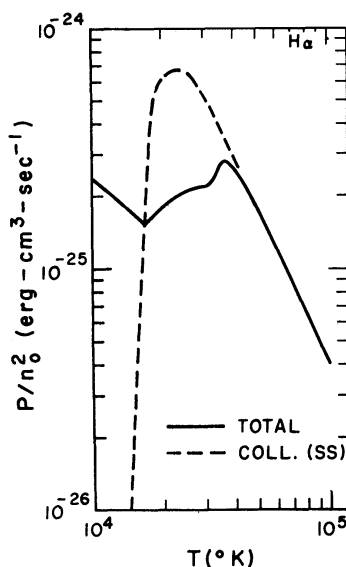


FIG. 10

FIG. 9.—Time-dependent  $L\alpha$  emission as a function of  $T$ . The line labeled “coll (time depend.)” gives the contribution of collisions to the  $L\alpha$  cooling, while the one labeled “recombin.” gives the contribution of recombinations; the dashed curve labeled “coll (SS)” gives the  $L\alpha$  emissivity when SS holds. The full curve is the sum of the two time-dependent terms.

FIG. 10.—Volume emissivity of  $H\alpha$  as a function of  $T$ . The curve labeled “total” gives the total  $H\alpha$  emission rate in the time-dependent case. The dashed curve labeled “coll. (SS)” gives the emissivity when SS holds. Both curves are computed in case B of Menzel (thick to the Lyman lines).

Figure 10 gives the volume emissivity of  $H\alpha$  as a function of  $T$  (40-eV case). The full curve labeled “total” gives the emissivity in the time-dependent case as given by equation (8), while the dashed curve labeled “coll. (SS)” gives the  $H\alpha$  emissivity when SS holds (from Parker 1964), both for case B of Baker and Menzel (1938).

The  $H\alpha$  emissivity is again less than the SS emissivity but not as much as with  $L\alpha$ , due to the fact that the second term in equation (8) is relatively more important than the corresponding term in the  $L\alpha$  emissivity. Below  $20,000^\circ\text{K}$ ,  $P_{H\alpha}$  is the same as the emissivity due to a radiatively excited nebula because  $P_{H\alpha}(\text{Recomb})$  is the only important term. At high temperatures ( $\geq 40,000^\circ\text{K}$ )  $P_{H\alpha}$  is the same as the emissivity in steady state, as is the case with  $L\alpha$ . As the temperature decreases, the hydrogen-line emissivities approach the emissivities of a radiatively excited nebula (cf. Burgess 1958), since at low temperatures the nebula is still mostly ionized, while the collisional excitation becomes negligible. We note that the Balmer decrement is not as steep as for nebulae that are collisionally excited; for  $T > 4 \times 10^4$  K the Balmer decrement is the collisional one which is approaching the Balmer decrement of a radiatively excited nebula as  $T$  increases (Baker and Menzel 1938). For  $T < 20,000^\circ\text{K}$  the cooling

region has a Balmer decrement like a radiatively excited nebula. In between ( $20,000 < T < 40,000^\circ \text{K}$ ) the Balmer decrement is not as steep as for a collisionally excited nebula (the SS case), but it is steeper than for a radiatively excited one. We conclude that radiatively cooling regions have a Balmer decrement not as steep as expected for a collisionally excited nebula (see also Cox 1972).

Figures 11–13 give the volume emissivity of  $L\alpha$  and  $H\alpha$ , as well as the forbidden lines [O II]  $\lambda\lambda 3726, 3729$ , [O III]  $\lambda\lambda 5007, 4959$ , [Ne III]  $\lambda\lambda 3869, 3968$ , and [Ne IV]  $\lambda 2440$ , as a function of time elapsed since the initial ionization in the 40-eV and 100-eV cases and as a function of time elapsed from a temperature of  $3.5 \times 10^5 \text{ K}$  in the SS,  $10^6 \text{ K}$  case. We see that the forbidden lines are much stronger than  $H\alpha$ , and even at  $T = 10^4 \text{ K}$  [O II], [O III] are a few times stronger than  $H\alpha$ . The exact relative intensities are of course different if different initial conditions are chosen, but the result that the Balmer lines are weak compared to the forbidden lines mentioned above is always true for radiatively cooling regions for  $T \geq 10^4 \text{ K}$ . Table 3 gives the ratio of the intensity of the [O II] line to that of the [O III] line. These calculations suggest the interesting possibility of using optical and ultraviolet line observations in addition to some independent temperature determination (e.g., through radio observations) to deduce the initial conditions of the cooling region. In certain cases the mere observation of a

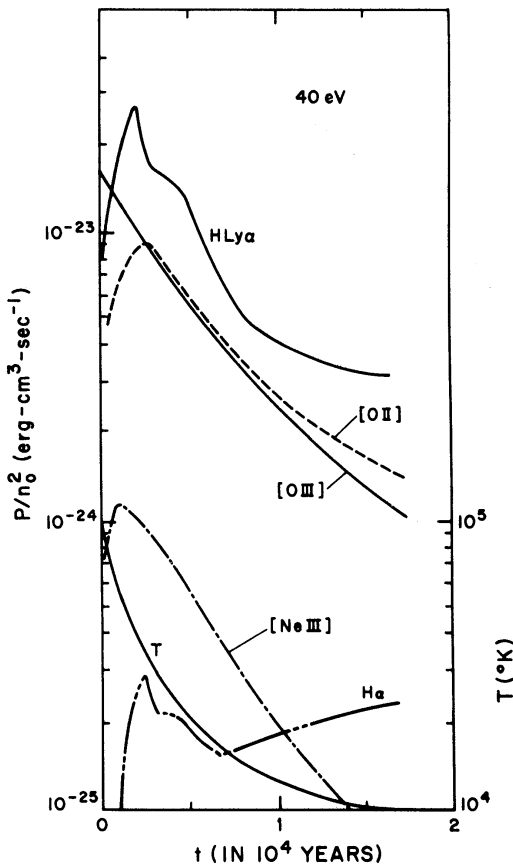


FIG. 11

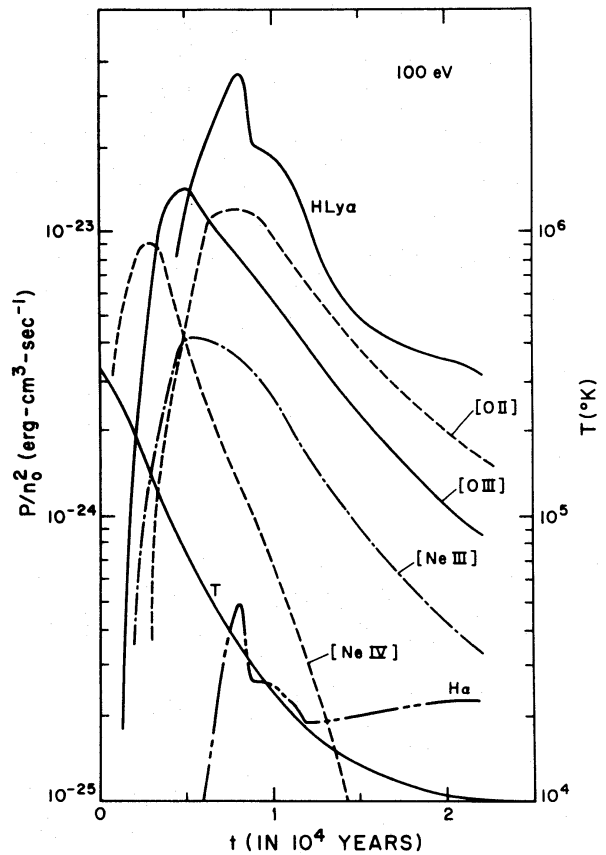


FIG. 12

FIG. 11.—Line emissivities in the 40-eV case as a function of time elapsed since the initial ionization;  $T$  is also shown.

FIG. 12.—Same as fig. 12 but in the 100-eV case.

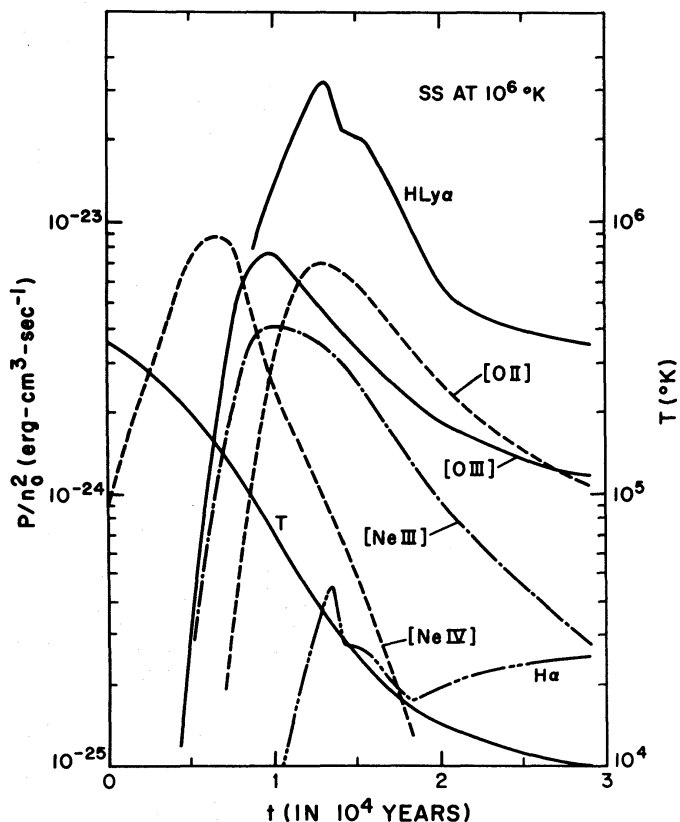


FIG. 13.—Line emissivities as a function of time  $t$  elapsed from a temperature of  $3.5 \times 10^5$  °K. SS,  $10^6$  °K case.

line can exclude a model; for instance, the observation of the [Ne IV] line would exclude the 40-eV burst.

Note that in diffuse emission nebulae—ionized by ultraviolet starlight—the forbidden lines of oxygen are very often strong, but rarely as strong or stronger than  $H\alpha$ . This is due to the fact that relatively low temperatures ( $5800$ – $7300$  °K) exist in those regions and the exponential factors in the forbidden-line emissivities drop fast as  $T$  decreases below  $10^4$  °K (see Pottasch 1965). There is, however, another important effect which occurs only for the regions examined here. Below about  $50,000$  °K (cf. table 3) the [O II] and [O III] lines have comparable intensities. This is due to delayed

TABLE 3  
LINE INTENSITY RATIO [O II]/[O III] AS A FUNCTION OF  $T$

$T$ (°K)	40 eV	100 eV	SS, $10^6$ °K
90,000.....	0.074	0.186	0.22
80,000.....	0.333	0.285	0.3
70,000.....	0.415	0.406	0.435
60,000.....	0.492	0.666	0.63
50,000.....	0.592	1.1	1.0
40,000.....	0.838	1.41	1.39
30,000.....	1.08	1.6	1.62
20,000.....	1.09	1.63	1.63
10,000.....	1.38	1.91	0.93



recombination. In H II regions ionized by starlight below  $10^4$  ° K, or in collisionally excited nebulae above  $10^4$  ° K, one of the two lines usually dominates, because the abundances of  $O^+$  and  $O^{++}$  are rarely comparable to each other at a given  $T$ .

We conclude that radiatively cooling regions are observable better in the forbidden lines than in the Balmer lines of hydrogen. Their spectrum is very different from that of a conventional diffuse emission nebula or a planetary nebula—i.e., radiatively excited nebulae—since  $H\alpha$  and  $H\beta$  are of negligible intensity compared to some forbidden lines of heavy elements. On the other hand, the Balmer decrement of a radiatively cooling region is not as steep as that of a collisionally excited nebula, and at low temperatures it is equal to the decrement of a radiatively excited nebula.

This work was carried out while I was doing my doctorate at MIT. I would like to thank A. Dalgarno, F. M. Flasar, H. Gerola, L. Sartori, J. Schwarz, and W. H. Tucker for useful discussions. Special thanks are due my thesis advisor P. Morrison for his help and encouragement, and R. A. McCray for introducing me to the idea of a time-dependent treatment, for long discussions, and for helping me with the present manuscript.

#### REFERENCES

- Allen, J. W., and Dupree, A. K. 1969, *Ap. J.*, **155**, 27.  
 Aller, L. H. 1961, *The Abundances of the Elements* (New York: Interscience Publishers).  
 Baker, J. G., and Menzel, D. H. 1938, *Ap. J.*, **88**, 52.  
 Brandt, J. C., Stecher, T. P., Crawford, D. L., and Maran, S. P. 1971, *Ap. J. (Letters)*, **163**, L99.  
 Burgess, A. 1958, *M.N.R.A.S.*, **118**, 477.  
 ———. 1965, *Ap. J.*, **141**, 1588.  
 Cox, D. P. 1970, unpublished Ph.D. thesis, University of California, San Diego.  
 ———. 1972, *Ap. J.*, **178**, 143.  
 Cox, D. P., and Daltabuit, E. 1971, *Ap. J.*, **167**, 113.  
 Cox, D. P., and Tucker, W. H. 1969, *Ap. J.*, **157**, 1157.  
 Field, G. B., and Steigman, G. 1971, *Ap. J.*, **166**, 59.  
 Gerola, H., Iglesias, E., and Gamba, Z. 1973, *Astron. and Ap.*, to be published.  
 House, L. L. 1964, *Ap. J. Suppl.*, **8**, 307.  
 Jura, M. 1971, unpublished Ph.D. thesis, Harvard University.  
 Jura, M., and Dalgarno, A. 1972, *Ap. J.*, **174**, 365.  
 Kafatos, M. C. 1971, in *The Gum Nebula and Related Problems*, ed., S. P. Maran, J. C. Brandt, and T. P. Stecher (Goddard Space Flight Center Report X-683-71-375), p. 110.  
 Kafatos, M. C., and Morrison, P. 1971, *Ap. J.*, **168**, 195.  
 Kafatos, M. C., and Tucker, W. H. 1972, *Ap. J.*, **175**, 837.  
 Kaplan, S. A., and Pikel'ner, S. B. 1971, *Interstellar Gas* (Cambridge, Mass.: Harvard University Press).  
 Lotz, W. 1967, *Ap. J. Suppl.*, **14**, 207.  
 Menzel, D. H. 1937, *Ap. J.*, **85**, 330.  
 Morrison, P., and Sartori, L. 1969, *Ap. J.*, **158**, 541.  
 Parker, R. A. R. 1964, *Ap. J.*, **139**, 208.  
 Pottasch, S. R. 1965, *Vistas in Astronomy*, **6**, 149.  
 Schwarz, J. 1972, *Ap. J.* (in press).  
 Seaton, M. J. 1959, *M.N.R.A.S.*, **119**, 81.  
 ———. 1960, *Rept. Progr. Phys.*, **23**, 313.  
 Spitzer, L. 1968, *Diffuse Matter in Space* (New York: Interscience Publishers).  
 Tarter, C. B. 1971, *Ap. J.*, **168**, 313.  
 Tucker, W. H., and Gould, R. J. 1966, *Ap. J.*, **144**, 244.  
 Tucker, W. H., and Koren, M. 1971, *Ap. J.*, **168**, 283.  
 Wiese, W. L., Smith, M. W., and Glennon, B. M. 1966, *Atomic Transition Probabilities*, Vol. 1, NSRDS.  
 Withbroe, G. 1971, *The Menzel Symposium*, ed., K. B. Gebbie, NBS Spec. Pub. No. 353 (Washington: U.S. Government Printing Office), p. 127.  
 Zanstra, H. 1927, *Ap. J.*, **65**, 50.

